Exceptional Entanglement Phenomena: Non-Hermiticity Meeting Nonclassicality

Pei-Rong Han,[1,*] Fan Wu,[1,*] Xin-Jie Huang,[1,*] Huai-Zhi Wu,[1] Chang-Ling Zou,[2,3,8] Wei Yi,[2,3,8] Mengzhen Zhang,[4] Hekang Li,[5] Kai Xu,[5,6,8] Dongning Zheng,[5,6,8] Heng Fan,[5,6,8] Jianming Wen,[7,†] Zhen-Biao Yang,[1,8,‡] and Shi-Biao Zheng[1,8,§]

[1]*Fujian Key Laboratory of Quantum Information and Quantum Optics, College of Physics and Information Engineering, Fuzhou University, Fuzhou, Fujian 350108, China*
[2]*CAS Key Laboratory of Quantum Information, University of Science and Technology of China, Hefei 230026, China*
[3]*CAS Center for Excellence in Quantum Information and Quantum Physics, University of Science and Technology of China, Hefei 230026, China*
[4]*Pritzker School of Molecular Engineering, University of Chicago, Chicago, Illinois 60637, USA*
[5]*Institute of Physics, Chinese Academy of Sciences, Beijing 100190, China*
[6]*CAS Center for Excellence in Topological Quantum Computation, University of Chinese Academy of Sciences, Beijing 100190, China*
[7]*Department of Physics, Kennesaw State University, Marietta, Georgia 30060, USA*
[8]*Hefei National Laboratory, Hefei 230088, China*

(Received 20 July 2023; accepted 15 November 2023; published 29 December 2023)

Non-Hermitian (NH) extension of quantum-mechanical Hamiltonians represents one of the most significant advancements in physics. During the past two decades, numerous captivating NH phenomena have been revealed and demonstrated, but all of which can appear in both quantum and classical systems. This leads to the fundamental question: what NH signature presents a radical departure from classical physics? The solution of this problem is indispensable for exploring genuine NH quantum mechanics, but remains experimentally untouched so far. Here, we resolve this basic issue by unveiling distinct exceptional entanglement phenomena, exemplified by an entanglement transition, occurring at the exceptional point of NH interacting quantum systems. We illustrate and demonstrate such purely quantum-mechanical NH effects with a naturally dissipative light-matter system, engineered in a circuit quantum electrodynamics architecture. Our results lay the foundation for studies of genuinely quantum-mechanical NH physics, signified by exceptional-point-enabled entanglement behaviors.

DOI: 10.1103/PhysRevLett.131.260201

When a physical system undergoes dissipation, the Hermiticity of its Hamiltonian dynamics is broken down. As any system inevitably interacts with its surrounding environment by exchanging particles or energy, non-Hermitian (NH) effects are ubiquitous in both classical and quantum physics. Such effects were once thought to be detrimental, and needed to be suppressed for observing physical phenomena of interest and for technological applications, until the discovery that NH effects could represent a complex extension of quantum mechanics [1–3]. Since then, increasing efforts have been devoted to the exploration of NH physics, leading to findings of many intriguing phenomena that are uniquely associated with NH systems. Most of these phenomena are closely related to the exceptional points (EPs), where both the eigenenergies and the eigenvectors of the NH Hamiltonian coalesce [4–6]. In addition to fundamental interest, such NH effects promise the realization of enhanced sensors [7–11].

Hitherto, there have been a plethora of experimental investigations on genuinely NH phenomena, ranging from real-to-complex spectral transition to NH topology [12–20], as well as on relevant applications [21–25], most of which were performed with classically interacting but nonentangled systems. The past few years have witnessed a number of demonstrations of similar NH phenomena in different quantum systems, ranging from photons [26–28] to atoms [29–31] and ions [32,33], and from nitrogen-vacancy centers [34–36] to superconducting circuits [37–39]. However, these experiments have been confined to realizations of NH semiclassical models, where the degree of freedom either of the light or of the matter was treated classically in the effective NH Hamiltonian describing the light-matter interaction, and consequently, the observed NH effects bear no relation to quantum entanglement. Indeed, all the genuinely NH effects demonstrated so far can occur in both quantum and classical systems. This naturally leads to an imperative issue: what feature can simultaneously manifest non-Hermiticity and nonclassicality? Recently, there has been a significant focus on nonequilibrium quantum phase transitions in the entanglement dynamics of NH many-body systems [40–42], but the purely quantum-mechanical NH features associated with the Hamiltonian eigenstates have remained unexplored.

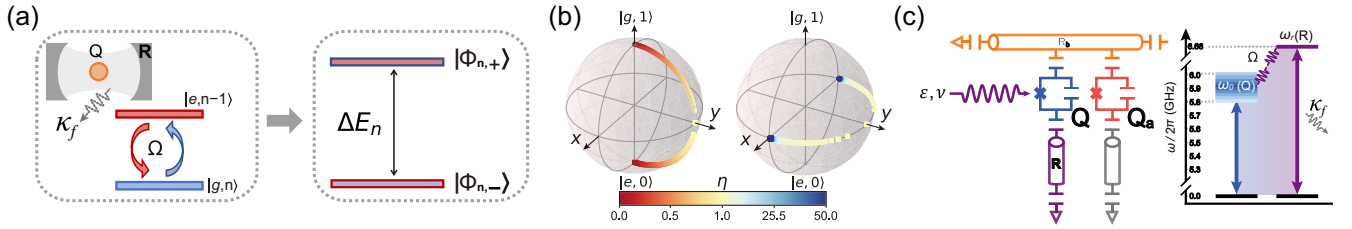

FIG. 1. NH light-matter interaction and experimental implementation. (a) Theoretical model. The system under investigation involves a quantized field mode with a decaying rate κ_f resonantly interacting with a matter qubit with a decaying rate κ_q. Their interaction is characterized by a coupling strength of Ω. The system's dynamics can be cast onto different U(1)-symmetric eigenspaces, denoted as $\{|e,n-1\rangle,|g,n\rangle\}$, within each of which there exist two eigenstates $|\Phi_{n,\pm}\rangle$, separated by a gap of ΔE_n. (b) Bloch representation of $|\Phi_{1,\pm}\rangle$ in the single-excitation subspace ($n=1$). For clarity, we here pictorially display the dependence of $|\Phi_{1,\pm}\rangle$ on the rescaled coupling strength $\eta=4\Omega/\kappa$. For $\eta=0$, $|\Phi_{1,\pm}\rangle$ correspond to $|e,0\rangle$ and $|g,1\rangle$, respectively. With the increase of η, $|\Phi_{1,\pm}\rangle$ are respectively rotated around $\pm x$ axes, and merged to the y axis at the EP $\eta=1$, featuring the occurrence of the maximally entangled state $|Y\rangle=(|g,1\rangle-i|e,0\rangle)/\sqrt{2}$. After crossing the EP, the eigenvectors $|\Phi_{1,\pm}\rangle$ remain on the equatorial plane, but are rotated around the z and $-z$ axes, progressively aligned with the $\pm x$ axes, tending to $|\pm X\rangle=(|g,1\rangle\pm|e,0\rangle)/\sqrt{2}$, respectively. (c) Implementation of the NH Hamiltonian. In the experimental system, a superconducting qubit Q is highly detuned from the lossy resonator R with a fixed frequency $\omega_r/2\pi=6.66$ GHz. The Q-R interaction is enabled with an ac flux, which modulates Q's energy gap around the mean value ω_0, with a frequency ν, mediating a photonic swapping coupling at one sideband, with the coupling strength controlled by the modulating amplitude ε.

We here perform an in-depth investigation on this fundamental problem, finding that dissipative interacting quantum systems can display exceptional entanglement phenomena. In particular, we discover an EP-induced entanglement transition, which represents a purely quantum-mechanical NH signature, with neither Hermitian nor classical analogs. We illustrate our discovery with a dissipative qubit-photon system, whose NH quantum effects are manifested by the singular entanglement behaviors of the bipartite entangled eigenstates. We experimentally demonstrated these singular behaviors in a circuit, where a superconducting qubit is controllably coupled to a decaying resonator. The exceptional entanglement signatures, inherent in the qubit-photon static eigenstates, are mapped out by a density matrix postcasting method, which enables us to extract the weak nonclassical signal from the strong noise background. In addition to the quantum character, the demonstrated NH phenomena originate from naturally occurring dissipation, distinct from that induced by an artificially engineered reservoir [12–39]. Our results are universal for composite quantum systems immersed in pervasive Markovian reservoirs, endowing NH quantum mechanics with genuinely nonclassical characters, which are absent in NH classical physics.

The theoretical model, used to illustrate the NH entanglement transition, is composed of a two-level system (qubit) resonantly coupled to a quantized photonic mode, as sketched in Fig. 1(a). The quantum state evolution trajectory without photon-number jumps is governed by the NH Hamiltonian (setting $\hbar=1$)

$$\mathcal{H}_{\rm NH}=\Omega(a^\dagger|g\rangle\langle e|+a|e\rangle\langle g|)-\frac{i}{2}\kappa_q|e\rangle\langle e|-\frac{i}{2}\kappa_f a^\dagger a, \quad (1)$$

where $|e\rangle$ ($|g\rangle$) denotes the upper (lower) level of the qubit, $a^\dagger$ (a) represents the creation (annihilation) operator for the photonic mode, κ_q (κ_f) is the energy dissipation rate for the qubit (field mode), and Ω is the qubit-field coupling strength. In the n-excitation subspace, the system has two right entangled eigenstates, given by

$$|\Phi_{n,\pm}\rangle=\mathcal{N}_{n,\pm}(\sqrt{n}\Omega|e,n-1\rangle+E_{n,\pm}|g,n\rangle), \quad (2)$$

where $\mathcal{N}_{n,\pm}=(n\Omega^2+|E_{n,\pm}|^2)^{-1/2}$ and $E_{n,\pm}=-i\gamma/4\pm\Delta E_n/2$ are the corresponding eigenenergies, with $\gamma=\kappa_f+\kappa_q$, $\Delta E_n=2\sqrt{n\Omega^2-\kappa^2/16}$, and $\kappa=\kappa_f-\kappa_q$. These two eigenstates are separated by an energy gap of ΔE_n. The inherent quantum entanglement makes the system fundamentally distinct from previously demonstrated NH semiclassical models [29–39], where the qubit is not entangled with the classical control field in any way. When $\Omega>\kappa/(4\sqrt{n})$, the system has a real energy gap, and undergoes Rabi-like oscillations, during which the qubit periodically exchanges a photon with the field mode. With the decrease of Ω, the energy gap is continuously narrowed until reaching the EP, where the two energy levels coalesce. After crossing the EP, the gap becomes imaginary, and the population evolution exhibits an overdamping feature.

Unlike previous investigations, here each eigenenergy is possessed by the two entangled components, neither of which has its own state. The nonclassical feature of each eigenstate is manifested by the light-matter entanglement, which can be quantified by the concurrence [43]

$$\mathcal{E}_\pm=\frac{2\sqrt{n}\Omega|E_{n,\pm}|}{|E_{n,\pm}|^2+n\Omega^2}. \quad (3)$$

When the rescaled coupling strength $\eta=4\sqrt{n}\Omega/\kappa$ is much smaller than 1, the two eigenstates are respectively

dominated by $|e, n-1\rangle$ and $|g, n\rangle$. With the increase of η, these two populations become increasingly balanced until reaching the EP $\eta = 1$, where both eigenstates converge to the same maximally entangled state. During this convergence, $\mathcal{E}_\pm$ exhibit a linear scaling with η. In the Bloch representation, this corresponds to a rotation of the eigenvector $|\Phi_{n,+}\rangle$ ($|\Phi_{n,-}\rangle$) around the x ($-x$) axis from pointing at the north (south) polar, until merging at the y axis, as shown in the left panel of Fig. 1(b). After crossing the EP, $\mathcal{E}_\pm$ become independent of Ω, which implies both two eigenstates keep maximally entangled. However, $|\Phi_{n,+}\rangle$ ($|\Phi_{n,-}\rangle$) is rotated around the z ($-z$) axis, progressively approaching the x ($-x$) axis [right panel of Fig. 1(b)]. This sudden switch of the rotation axis manifests an entanglement transition at the EP, where the derivative of the concurrence with respect to η presents a discontinuity, jumping from 1 to 0. By measuring the time-evolving output states associated with the no-jump trajectory, we can extract the information about both the energy gap and entanglement regarding the "static" eigenstates. It should be noted that the resonator plays a radically different role from the ancilla used in the previous experiments [34–37], which was introduced as an artificially engineered environment to the test qubit, but whose dynamics was not included in the effective NH Hamiltonian dynamics. In distinct contrast, in the present system the degree of freedom of R constitutes a part of the Hamiltonian, whose NH term is induced by the natural environment.

The experimental demonstration of the NH physics is performed in a circuit quantum electrodynamics architecture, where the qubit-photon model is realized with a superconducting qubit Q and its resonator R with a fixed frequency $\omega_r/2\pi = 6.66$ GHz (see Supplemental Material, Sec. S2 [44]). The decaying rates of Q and R are $\kappa_q \simeq 0.07$ MHz and $\kappa_f = 5$ MHz, respectively. The accessible maximum frequency of Q, $\omega_{\max} = 2\pi \times 6.01$ GHz, is lower than ω_r by an amount much larger than their on-resonance swapping coupling $g_r = 2\pi \times 41$ MHz [Fig. 1(c)]. To observe the EP physics, an ac flux is applied to Q, modulating its frequency as $\omega_q = \omega_0 + \varepsilon\cos(\nu t)$, where ω_0 is the mean $|e\rangle - |g\rangle$ energy difference, and ε and ν denote the modulating amplitude and frequency. This modulation enables Q to interact with R at a preset sideband, with the photon swapping rate Ω tunable by ε (see Supplemental Material, Sec. S3 [44]).

Our experiment focuses on the single-excitation case ($n = 1$). Before the experiment, the system is initialized to the ground state $|g, 0\rangle$. The experiment starts by transforming Q from the ground state $|g\rangle$ to excited state $|e\rangle$ with a π pulse, following which the parametric modulation is applied to Q to initiate the Q-R interaction (see Fig. S4 of Supplemental Material for the pulse sequence). This interaction, together with the natural dissipations, realizes the NH Hamiltonian of Eq. (1). After the modulating pulse, the Q-R state is measured with the assistance of an ancilla qubit (Q_a) and a bus resonator (R_b), which is coupled to both Q and Q_a. The subsequent $Q \to R_b$, $R_b \to Q_a$, and $R \to Q$ quantum state transferring operations map the Q-R output state to the Q_a-Q system, whose state can be read out by quantum state tomography (see Supplemental Material, Sec. S5 [44]).

A defining feature of our system is the conservation of the excitation number under the NH Hamiltonian. This Hamiltonian evolves the system within the subspace $\{|e, 0\rangle, |g, 1\rangle\}$. A quantum jump would disrupt this conversion, moving the system out of this subspace. This property in turn enables us to postselect the output state governed the NH Hamiltonian simply by discarding the joint Q_a-Q outcome $|g, g\rangle$ after the state mapping. With a correction of the quantum state distortion caused by the decoherence occurring during the state mapping, we can infer the quantum Rabi oscillatory signal, characterized by the evolution of the joint probability $|e, 0\rangle$, denoted as $P_{e,0}$. Figure 2(a) shows thus-obtained $P_{e,0}$ as a function of the rescaled coupling η and the Q-R interaction time t. The results clearly show that both the shapes and periods of vacuum Rabi oscillations are significantly modulated by the NH term around the EP $\eta = 1$, where incoherent dissipation is comparable to the coherent interaction. These experimental results are in good agreement with numerical simulations (see Supplemental Material, Sec. S4 [44]).

The Rabi signal does not unambiguously reveal the system's quantum behavior. To extract full information of the two-qubit entangled state, it is necessary to individually measure all three Bloch vectors for each qubit, and then correlate the results for the two qubits. The z component can be directly measured by state readout, while measurements of the x and y components require y rotations and x rotations before state readout, which breaks down excitation-number conservation, and renders it impossible to distinguish individual jump events from no-jump ones. We circumvent this problem by first reconstructing the two-qubit density matrix using all the measurement outcomes, and then discarding the matrix elements associated with $|g, g\rangle$ (see Supplemental Material, Sec. S5 [44]). This effectively postcasts the two-qubit state to the subspace $\{|e, g\rangle, |g, e\rangle\}$. We note that such a technique is in sharp contrast with the conventional postselection method, where some auxiliary degree of freedom (e.g., propagation direction of a photon) enables reconstruction of the relevant conditional output state, but which is unavailable in the NH qubit-photon system. With a proper correction for the state mapping error, we obtain the Q-R output state governed by the non-Hermitian Hamiltonian. In Fig. 2(b), we present the resulting Q-R concurrence, as a function of η and t. To show the entanglement behaviors more clearly, we present the concurrence evolutions for $\eta = 5$ and 0.5 in Figs. 2(c) and 2(d), respectively. The results demonstrate that the entanglement exhibits distinct evolution patterns in the regimes above and below the EP.

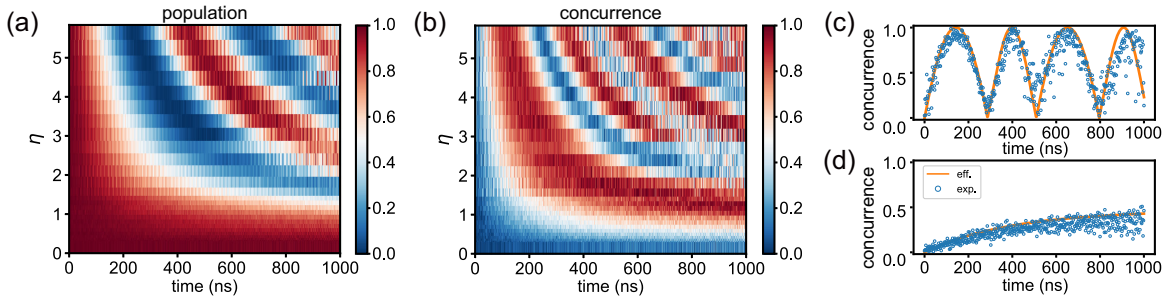

FIG. 2. Characterization of NH dynamical evolutions. (a) Measured evolutions of the population $|e,0\rangle$ for different values of the rescaled coupling η. The signals are extracted by correlating the measurement outcomes of Q and Q_a, which correspond to the outputs of R and Q right before the state mappings. The NH Hamiltonian evolution trajectory is postselected by discarding the detection events $|g,g\rangle$, and renormalizing the remaining outcomes $|g,e\rangle$ and $|e,g\rangle$. (b) Evolutions of the concurrences for different values of η. The concurrence at each point is inferred with the postprojected density matrix, obtained by reconstructing the output Q-Q_a density matrix, projecting the thus-obtained two-qubit state to the reduced subspace with one excitation, and then renormalizing the remaining matrix elements. (c),(d) Concurrence evolutions for $\eta = 5$ (c) and 0.5 (d). The orange solid curves are the numerical simulations using the effective Hamiltonian and the blue circles are the experimental results.

To reveal the close relation between the exceptional entanglement behavior and the EP, we infer the eigenvalues and eigenstates of the NH Hamiltonian from the output states, measured for different evolution times (see Supplemental Material, Sec. S7 [44]). The concurrences associated with the two eigenstates, obtained for different values of η, are shown in Figs. 3(a) and 3(b) (dots), respectively. As expected, each of these entanglements exhibits a linear scaling below the EP, but is saturated at the EP, and no longer depends upon η after crossing the EP. The singular features around the EP are manifested by their derivatives to η, which are shown in the insets. The discontinuity of these derivatives indicates the occurrence of an entanglement transition at the EP. Such a nonclassical behavior, as a consequence of the competition between the coherent coupling and incoherent dissipation, represents a unique character of strongly correlated NH quantum systems, but has not been reported so far. These results demonstrate a longitudinal merging of the two entangled eigenstates at the EP [left panel of Fig. 2(b)]. Accompanying this is the onset of the transverse splitting, which can be characterized by the relative phase difference between $|\Phi_{1,\pm}\rangle$, defined as $\varphi = \varphi_+ - \varphi_-$, with $\varphi_\pm$ representing the relative phases between $|g,1\rangle$ and $|e,0\rangle$ in the eigenstates $|\Phi_{1,\pm}\rangle$. Such a phase difference, inferred for different values of η, is displayed in Fig. 3(c). This quantum-mechanical NH signature is universally applicable to dissipative interacting quantum systems, a feature absent in earlier superconducting-circuit-based single-qubit NH experiments [38,39].

The demonstrated exceptional entanglement transition is a purely quantum-mechanical NH effect. On one hand, quantum entanglement, which has no classical analogs, represents a most characteristic trait that distinguishes quantum physics from classical mechanics [50]. On the other hand, this effect, uniquely associated with the EP, is absent in Hermitian qubit-photon systems [51–54]. We further note that such an NH effect can occur in other dissipative quantum-mechanically correlated systems, e.g., a system composed of two or more coupled qubits with unbalanced decaying rates (see Supplemental Material,

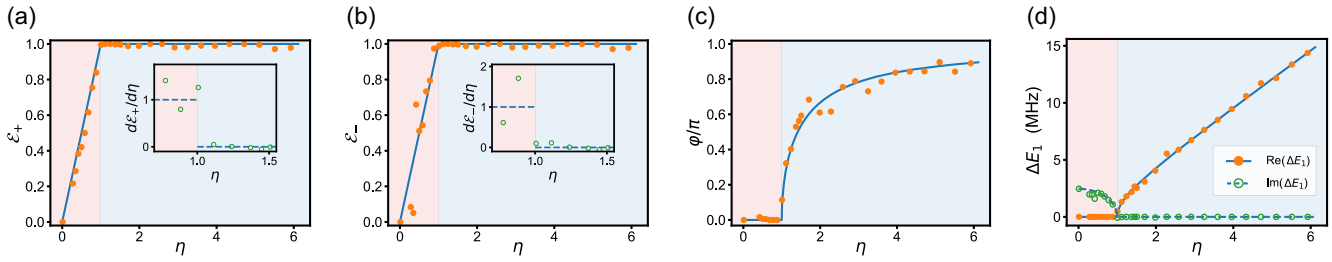

FIG. 3. Observation of exceptional phase transitions. (a),(b) Entanglements for the eigenstates $|\Phi_{1,+}\rangle$ and $|\Phi_{1,-}\rangle$ versus η. We obtain the concurrences $\mathcal{E}_\pm$ at each point based on the corresponding eigenstates, which are mapped out from the Q-R output states, measured for different evolution times. The dots denote the inferred concurrences, which well agree with the results for the ideal output states. The derivatives $d\mathcal{E}_\pm/d\eta$ around the EP, obtained by $[\mathcal{E}_\pm(\eta+\delta\eta) - \mathcal{E}_\pm(\eta)]/\delta\eta$, are displayed in the insets. (c) Relative phase difference (φ) between $|\Phi_{1,\pm}\rangle$. This phase difference is defined as $\varphi = \varphi_+ - \varphi_-$, where $\varphi_\pm$ are the relative phase between $|g,1\rangle$ and $|e,0\rangle$ in the eigenstates $|\Phi_{1,\pm}\rangle$. (d) Spectral gap ΔE_1. As the eigenspectrum is possessed by the entangled eigenstates of the Q-R system, this gap corresponds to the vacuum Rabi splitting. The solid and dashed lines denote the real and imaginary parts, respectively.

Sec. S8 [44]). This implies that such a quantum-mechanical NH signature is universal for dissipative interacting quantum systems.

The real and imaginary parts of the extracted quantum Rabi splitting ΔE_n are shown in Fig. 3(d). As theoretically predicted, above the EP the two eigenenergies have a real gap, which is continuously narrowed when the control parameter η is decreased until reaching the EP, where the two levels coalesce. After crossing the EP, the two levels are resplit but with an imaginary gap, which increases when η is decreased. This corresponds to the real-to-imaginary transition of the vacuum Rabi splitting between the Q-R entangled eigenstates, which is in distinct contrast with the previous experiments on $\mathcal{PT}$ symmetry breaking [29–39], realized with the semiclassical models, where the exceptional physics has no relation with quantum entanglement.

In conclusion, we have discovered an exceptional entanglement transition in a fundamental light-matter system governed by an NH Hamiltonian, establishing a close connection between quantum correlations and non-Hermitian effects. This transition has neither Hermitian nor classical analogs, representing the unique feature of NH quantum mechanics. The experimental demonstration is performed in a circuit, where a superconducting qubit is controllably coupled to a resonator with a non-negligible dissipation induced by a natural Markovian reservoir. The NH quantum signatures of the eigenstates are inferred from the no-jump output state, measured for different evolution times. Our results push NH Hamiltonian physics from the classical to genuinely nonclassical regime, where the emergent phenomena have neither Hermitian nor classical analogs. The postprojection method, developed for extracting the no-jump output density matrix, would open the door to experimentally explore purely quantum-mechanical NH effects in a broad spectrum of interacting systems, where excitation number is initially definite and conserved under the NH Hamiltonian. Such systems include resonator-qubit arrays [55], fully connected architectures involving multiple qubits coupled to a single resonator [56], and lattices composed of many qubits with nearest-neighbor coupling [57]. When the system initially has n excitations, the no-jump trajectory can be postselected by discarding the outcomes with less than n excitations.

We thank Liang Jiang at University of Chicago for valuable comments. This work was supported by the National Natural Science Foundation of China (Grants No. 12274080, No. 11875108, No. 12204105, No. 11774058, No. 12174058, No. 11974331, No. 11934018, No. 92065114, and No. T2121001), Innovation Program for Quantum Science and Technology (Grants No. 2021ZD0300200 and No. 2021ZD0301200), NSF (Grant No. 2329027), the Strategic Priority Research Program of Chinese Academy of Sciences (Grant No. XDB28000000), the National Key R&D Program under (Grant No. 2017YFA0304100), the Key-Area Research and Development Program of Guangdong Province, China (Grant No. 2020B0303030001), Beijing Natural Science Foundation (Grant No. Z200009), and the Project from Fuzhou University (Grant No. 049050011050).

S. B. Z. predicted the exceptional entanglement transition and conceived the experiment. P. R. H. and X. J. H., supervised by Z. B. Y. and S. B. Z., carried out the experiment. F. W., P. R. H., J. W., and S. B. Z. analyzed the data. S. B. Z., J. W., Z. B. Y., and W. Y. cowrote the Letter. All authors contributed to interpretation of observed phenomena and helped to improve presentation of the Letter.

*These authors contributed equally to this work.
†Corresponding author: jianming.wen@gmail.com
‡Corresponding author: zbyang@fzu.edu.cn
§Corresponding author: t96034@fzu.edu.cn

[1] C. M. Bender and S. Boettcher, Real spectra in non-Hermitian Hamiltonians having $\mathcal{PT}$ symmetry, Phys. Rev. Lett. **80**, 5243 (1998).
[2] C. M. Bender, D. C. Brody, and H. F. Jones, Complex extension of quantum mechanics, Phys. Rev. Lett. **89**, 270401 (2002).
[3] N. Moiseyev, *Non-Hermitian Quantum Mechanics* (Cambridge University Press, Cambridge, England, 2011).
[4] Ş. K. Özdemir, S. Rotter, F. Nori, and L. Yang, Parity–time symmetry and exceptional points in photonics, Nat. Mater. **18**, 783 (2019).
[5] E. J. Bergholtz, J. C. Budich, and F. K. Kunst, Exceptional topology of non-Hermitian systems, Rev. Mod. Phys. **93**, 015005 (2021).
[6] K. Ding, C. Fang, and G. Ma, Non-Hermitian topology and exceptional-point geometries, Nat. Rev. Phys. **4**, 745 (2022).
[7] Z.-P. Liu, J. Zhang, Ş. K. Özdemir, B. Peng, H. Jing, X.-Y. Lü, C.-W. Li, L. Yang, F. Nori, and Y.-X Liu, Metrology with $\mathcal{PT}$-symmetric cavities: Enhanced sensitivity near the $\mathcal{PT}$-phase transition, Phys. Rev. Lett. **117**, 110802 (2016).
[8] M. Zhang, W. Sweeney, C. W. Hsu, L. Yang, A. D. Stone, and L. Jiang, Quantum noise theory of exceptional point amplifying sensors, Phys. Rev. Lett. **123**, 180501 (2019).
[9] Y. Chu, Y. Liu, H. Liu, and J. Cai, Quantum sensing with a single-qubit pseudo-Hermitian system, Phys. Rev. Lett. **124**, 020501 (2020).
[10] X.-W Luo, C. Zhang, and S. Du, Quantum squeezing and sensing with pseudo anti-parity-time symmetry, Phys. Rev. Lett. **128**, 173602 (2022).
[11] J. Wang, D. Mukhopadhyay, and G. S. Agarwal, Quantum Fisher information perspective on sensing in anti-PT symmetric systems, Phys. Rev. Res. **4**, 013131 (2022).
[12] C. Dembowski, H.-D. Gräf, H. L. Harney, A. Heine, W. D. Heiss, H. Rehfeld, and A. Richter, Experimental observation of the topological structure of exceptional points, Phys. Rev. Lett. **86**, 787 (2001).
[13] Y. Choi, S. Kang, S. Lim, W. Kim, J.-R. Kim, J.-H. Lee, and K. An, Quasieigenstate coalescence in an atom-cavity quantum composite, Phys. Rev. Lett. **104**, 153601 (2010).

[14] T. Gao *et al.*, Observation of non-Hermitian degeneracies in a chaotic exciton-polariton billiard, Nature (London) **526**, 554 (2015).
[15] D. Zhang, X.-Q. Luo, Y.-P. Wang, T.-F. Li, and J. Q. You, Observation of the exceptional point in cavity magnon-polaritons, Nat. Commun. **8**, 1368 (2017).
[16] F. E. Öztürk, T. Lappe, G. Hellmann, J. Schmitt, J. Klaers, and F. Vewinger, Observation of a non-Hermitian phase transition in an optical quantum gas, Science **372**, 88 (2021).
[17] W. Tang, X. Jiang, K. Ding, Y.-X. Xiao, Z.-Q. Zhang, C. T. Chan, and G. Ma, Exceptional nexus with a hybrid topological invariant, Science **370**, 1077 (2020).
[18] K. Wang, A. Dutt, K. Y. Yang, C. C. Wojcik, J. Vučković, and S. Fan, Generating arbitrary topological windings of a non-Hermitian band, Science **371**, 1240 (2021).
[19] K. Wang, A. Dutt, C. C. Wojcik, and S. Fan, Topological complex-energy braiding of non-Hermitian bands, Nature (London) **598**, 59 (2021).
[20] Y. S. S. Patil, J. Höller, P. A. Henry, C. Guria, Y. Zhang, L. Jiang, N. Kralj, N. Read, and J. G. E. Harris, Measuring the knot of non-Hermitian degeneracies and non-commuting braids, Nature (London) **607**, 271 (2022).
[21] J. Doppler, A. A. Mailybaev, J. Böhm, U. Kuhl, A. Girschik, F. Libisch, T. J. Milburn, P. Rabl, N. Moiseyev, and S. Rotter, Dynamically encircling an exceptional point for asymmetric mode switching, Nature (London) **537**, 76 (2016).
[22] H. Xu, D. Mason, L. Jiang, and J. G. E. Harris, Topological energy transfer in an optomechanical system with exceptional points, Nature (London) **537**, 80 (2016).
[23] J. W. Yoon *et al.*, Time-asymmetric loop around an exceptional point over the full optical communication band, Nature (London) **562**, 86 (2018).
[24] W. Chen, Ş. K. Özdemir, G. Zhao, J. Wiersig, and L. Yang, Exceptional points enhance sensing in an optical microcavity, Nature (London) **548**, 192 (2017).
[25] H. Hodaei, A. U. Hassan, S. Wittek, H. Garcia-Gracia, R. El-Ganainy, D. N. Christodoulides, and M. Khajavikhan, Enhanced sensitivity at higher-order exceptional points, Nature (London) **548**, 187 (2017).
[26] S. Yu *et al.*, Experimental investigation of quantum $\mathcal{PT}$-enhanced sensor, Phys. Rev. Lett. **125**, 240506 (2020).
[27] K. Wang, L. Xiao, J. C. Budich, W. Yi, and P. Xue, Simulating exceptional non-Hermitian metals with single-photon interferometry, Phys. Rev. Lett. **127**, 026404 (2021).
[28] Y.-L. Fang, J.-L. Zhao, Y. Zhang, D.-X. Chen, Q.-C. Wu, Y.-H. Zhou, C.-P. Yang, and F. Nori, Experimental demonstration of coherence flow in PT- and anti-PT-symmetric systems, Commun. Phys. **4**, 223 (2021).
[29] P. Peng, W. Cao, C. Shen, W. Qu, J. Wen, L. Jiang, and Y. Xiao, Anti-parity-time symmetry with flying atoms, Nat. Phys. **12**, 1139 (2016).
[30] J. Li, A. K. Harter, J. Liu, L. d. Melo, Y. N. Joglekar, and L. Luo, Observation of parity-time symmetry breaking transitions in a dissipative Floquet system of ultracold atoms, Nat. Commun. **10**, 855 (2019).
[31] Z. Ren, D. Liu, E. Zhao, C. He, K. K. Pak, J. Li, and G.-B. Jo, Chiral control of quantum states in non-Hermitian spin-orbit-coupled fermions, Nat. Phys. **18**, 385 (2022).
[32] W.-C. Wang *et al.*, Observation of $\mathcal{PT}$-symmetric quantum coherence in a single-ion system, Phys. Rev. A **103**, L020201 (2021).
[33] L. Ding, K. Shi, Q. Zhang, D. Shen, X. Zhang, and W. Zhang, Experimental determination of $\mathcal{PT}$-symmetric exceptional points in a single trapped ion, Phys. Rev. Lett. **126**, 083604 (2021).
[34] Y. Wu, W. Liu, J. Geng, X. Song, X. Ye, C. K. Duan, X. Rong, and J. F. Du, Observation of parity-time symmetry breaking in a single-spin system, Science **364**, 878 (2019).
[35] W. Liu, Y. Wu, C.-K. Duan, X. Rong, and J. Du, Dynamically encircling an exceptional point in a real quantum system, Phys. Rev. Lett. **126**, 170506 (2021).
[36] W. Zhang, X. Ouyang, X. Huang, X. Wang, H. Zhang, Y. Yu, X. Chang, Y. Liu, D.-L. Deng, and L.-M. Duan, Observation of non-Hermitian topology with nonunitary dynamics of solid-state spins, Phys. Rev. Lett. **127**, 090501 (2021).
[37] S. Dogra, A. A. Melnikov, and G. S. Paraoanu, Quantum simulation of parity-time symmetry breaking with a superconducting quantum processor, Commun. Phys. **4**, 26 (2021).
[38] M. Naghiloo, M. Abbasi, Y. N. Joglekar, and K. W. Murch, Quantum state tomography across the exceptional point in a single dissipative qubit, Nat. Phys. **15**, 1232 (2019).
[39] Z. Wang, Z. Xiang, T. Liu, X. Song, P. Song, X. Guo, L. Su, H. Zhang, Y. Du, and D. Zheng, Observation of the exceptional point in superconducting qubit with dissipation controlled by parametric modulation, Chin. Phys. B **30**, 100309 (2021).
[40] K. Kawabata, T. Numasawa, and S. Ryu, Entanglement phase transition induced by the non-Hermitian skin effect, Phys. Rev. X **13**, 021007 (2023).
[41] X. Turkeshi and M. Schiró, Entanglement and correlation spreading in non-Hermitian spin chains, Phys. Rev. B **107**, L020403 (2023).
[42] Y. L. Gal, X. Turkeshi, and M. Schiró, Volume-to-area law entanglement transition in a non-Hermitian free fermionic chain, SciPost Phys. **14**, 138 (2023).
[43] W. K. Wootters, Entanglement of formation of an arbitrary state of two qubits, Phys. Rev. Lett. **80**, 2245 (1998).
[44] See Supplemental Material at http://link.aps.org/supplemental/10.1103/PhysRevLett.131.260201 for detailed calculations of the concurrences and negativities for the eigenstates and NH-Hamiltonian-evolved states, a description of system parameters, a derivation of the effective Q-R interaction Hamiltonian, numerical simulations of the NH Hamiltonian dynamics, discussions of measurement of the Q-R output state and of extraction of the NH Hamiltonian eigenenergies and eigenstates, as well as an investigations on the exceptional entanglement transition in a two-qubit system, which includes Refs. [43,45–49].
[45] R. Horodecki, P. Horodecki, M. Horodecki, and K. Horodecki, Quantum entanglement, Rev. Mod. Phys. **81**, 865 (2009).
[46] S.-B. Zheng and G.-C. Guo, Efficient scheme for two-atom entanglement and quantum information processing in cavity QED, Phys. Rev. Lett. **85**, 2392 (2000).
[47] S. Osnaghi, P. Bertet, A. Auffeves, P. Maioli, M. Brune, J. M. Raimond, and S. Haroche, Coherent control of an

atomic collision in a cavity, Phys. Rev. Lett. **87**, 037902 (2001).
[48] C. Song, K. Xu, W. Liu, C.-P. Yang, S.-B. Zheng, H. Deng *et al.*, 10-qubit entanglement and parallel logic operations with a superconducting circuit, Phys. Rev. Lett. **119**, 180511 (2017).
[49] Y. Zhou *et al.*, Rapid and unconditional parametric reset protocol for tunable superconducting qubits, Nat. Commun. **12**, 5924 (2021).
[50] V. Vedral, Quantum entanglement, Nat. Phys. **10**, 256 (2014).
[51] R. J. Thompson, G. Rempe, and H. J. Kimble, Observation of normal-mode splitting for an atom in an optical cavity, Phys. Rev. Lett. **68**, 1132 (1992).
[52] F. Bernardot, P. Nussenzveig, M. Brune, J. M. Raimond, and S. Haroche, Vacuum Rabi splitting observed on a microscopic atomic sample in a microwave cavity, Europhys. Lett. **17**, 33 (1992).
[53] J. M. Fink, M. Goppl, M. Baur, R. Bianchetti, P. J. Leek, A. Blais, and A. Wallraff, Climbing the Jaynes-Cummings ladder and observing its nonlinearity in a cavity QED system, Nature (London) **454**, 315 (2008).
[54] L. S. Bishop, J. M. Chow, J. Koch, A. A. Houck, M. H. Devoret, E. Thuneberg, S. M. Girvin, and R. J. Schoelkopf, Nonlinear response of the vacuum Rabi resonance, Nat. Phys. **5**, 105 (2009).
[55] M. Mariantoni *et al.*, Photon shell game in three-resonator circuit quantum electrodynamics, Nat. Phys. **7**, 287 (2011).
[56] C. Song *et al.*, Generation of multicomponent atomic Schrödinger cat states of up to 20 qubits, Science **365**, 574 (2019).
[57] M. Gong *et al.*, Quantum walks on a programmable two-dimensional 62-qubit superconducting processor, Science **372**, 948 (2021).